# Impact Assessment of Plug-in Electric Vehicle Charging Locations on Power Systems with Integrated Wind Farms Incorporating Dynamic Thermal Limits

Bader Alharbi and Dilan Jayaweera

***Abstract*—The increased presence of electric vehicle charging locations in a power system with high penetration of intermittent wind power potentially leads to operation complexities resulting in abnormal impacts. This paper proposes an innovative framework for assessing the impact of plug-in electric vehicle (PEV) charging locations on a power system with integrated wind farms, incorporating dynamic thermal limits (DTLs). The framework comprises Monte Carlo simulation, which is embedded with stochastic modeling of various uncertainties under the key operating conditions. As part of the modeling framework, the transmission lines are ranked in accordance with the lowest level of expected energy not supplied. The PEV charging demand is then modeled by incorporating DTLs and applied to the least stressed transmission lines, following the IEEE 738-2006 standard. The new assessment framework is investigated using an IEEE 24-bus test system. The results demonstrate that applying DTLs on the least stressed transmission lines in conjunction with the integration of decentralized wind farms and strategic charging location of PEVs significantly improves the security of the energy supply and considerably reduces interruption costs, as opposed to not having such a framework.**

***Index Terms*—Dynamic thermal limit, impact assessment, Monte Carlo simulation, plug-in electric vehicles, wind farms.**

## I. Introduction

With the significant development of plug-in electric vehicles (PEVs) and related government support policies, PEVs have become more attractive to consumers. The rapid rise in PEV use has been accompanied by new concerns for modern power systems due to many uncertainties associated with the timing of charging station use and the substantial demand linked to PEVs, which can place further stress on power transmission lines. Power transmission systems are generally operated based on static thermal limits (STLs), but can be run using dynamic thermal limits (DTLs); this may vary transmission line ratings as they are based on real-time environmental and operating conditions [1] - [3]. DTL represents the real-time thermal limit and is used to determine the temporary operating capacity of a transmission line. The operating capacity of a transmission line is dependent on a multitude of factors, and the temperature of conductors, ambient temperature, and wind speed are among the most important factors. Usually, the transmission lines are designed by considering standard/fixed conditions; however, these conditions vary in real-world situations, which could result in varied operating capacity of the transmission line. The main influential factors for DTL calculations are weather conditions such as the wind speed, ambient temperature, and wind direction and line characteristics such as the line loading, conductor temperature, and conductor sag. DTL facilitates the use of the extra capacity of a transmission line in a real power grid under favorable conditions [3]. The calculated DTL is higher than the STL under favorable conditions on a transmission line [4].

Recently, an increasing number of studies on DTLs have been published. For example, in the work reported in [5], the reliability was assessed by considering DTLs and optimal conditions in a power grid. The IEEE 738-2006 standard in [6] was employed in [5] to calculate the DTLs for a variety of weather conditions, with 200% greater DTLs being observed in some areas. A risk assessment approach that involved the application of DTLs to transmission lines, based on the loading severity index, was proposed in [7].

The literature also contains a significant quantity of research devoted to examining the impact of PEVs on modern power systems, from several perspectives. A probabilistic approach was proposed to evaluate the daily effects on the power grid associated with PEV parking lots [8]. The impact of different PEV charging modes on the reliability of a modern power system was examined in [9]. The work presented in [10] proposed a reliability assessment approach that con-

Manuscript received: July 5, 2020; revised: December 20, 2020; accepted: April 8, 2021. Date of CrossCheck: April 8, 2021. Date of online publication: May 7, 2021.

This research was conducted at the University of Birmingham, UK, and was financially supported by Majmaah University and the Ministry of Education in Saudi Arabia.

This article is distributed under the terms of the Creative Commons Attribution 4.0 International License (http://creativecommons.org/licenses/by/4.0/).

B. Alharbi (corresponding author) is with the Department of Electronic, Electrical and Systems Engineering, University of Birmingham, Birmingham, UK, and he is also with the Department of Electrical Engineering, College of Engineering in Majmaah University, Al-Majmaah 11952, Saudi Arabia (e-mail: BXA591@bham.ac.uk).

D. Jayaweera is with the Department of Electronic, Electrical and Systems Engineering, University of Birmingham, Birmingham, UK (e-mail: D. Jayaweera@bham.ac.uk).

DOI: 10.35833/MPCE.2020.000445

sidered a variety of PEV charging models. An approach for the risk assessment of plug-in hybrid electric vehicles embedded in an active distribution network was proposed in [11]. Different energy management strategies for PEVs in a distribution network were studied in [12]. A reliability assessment approach for PEVs considering the demand response in a distribution network was proposed in [13]. While many studies have been conducted to assess the impact of PEV charging demand or the use of DTLs on power transmission systems, no previous study has investigated the impact of PEV charging on the least stressed transmission lines while applying DTLs in the presence of large wind farms.

We aim to assess the strategic impact of PEV charging from the least stressed locations in a power system, with the application of DTLs and the integration of large wind farms. The expected energy not supplied (EENS) and expected interruption cost (EIC) values are considered to assess the associated impacts.

The contributions of this study are: ① a new framework is proposed to employ power system stress as a means of identifying the least stressed transmission lines; ② an impact evaluation framework is introduced, which includes the consideration of the ranking of power system stress with the integration of large wind systems and the application of DTLs on a power transmission system, with respect to the PEV charging locations; ③ an advanced framework for the impact assessment of a power system with strategic charging of PEVs through less stressed charging stations considering PEV mobility benefits is proposed.

The remainder of this paper is organized as follows. Section II introduces the proposed framework. Section III details the implementation of the frameworks through case studies, and Section IV provides the conclusions.

## II. Proposed Framework

The proposed framework comprises two stages: the first involves ranking the stress on the transmission lines in the power system and the second assesses the impact associated with the strategic selection of PEV charging locations with the application of DTLs on the transmission lines and integrated large wind farms. The Monte Carlo simulation in the first stage of the proposed framework is shown in Fig. 1, where ENS stands for energy not supplied. The base-case system with the related technical data is modeled first to evaluate the base-case feasibility of the method [14]. Each instance of line tripping is sequentially simulated. Then, the relevant centralized or decentralized wind farms are integrated. At the connected buses of the transmission line, PEV demand systems (if any) are incorporated, followed by the simulation of the outage of components based on failure rates. Next, the power flow is conducted to evaluate the technical feasibility of the test system. A corrective control is then performed to avoid any divergence or constraint violations as appropriate. If there are no violations, the procedure is run for all sample trials of the Monte Carlo simulation until it establishes convergence, following which, the EENS value is estimated. Next, the procedure is repeated at alternate charging station locations. After all the effective lines are considered for assessment and the EENS for each case is obtained using a Monte Carlo simulation, the transmission lines are ranked based on the EENS values.

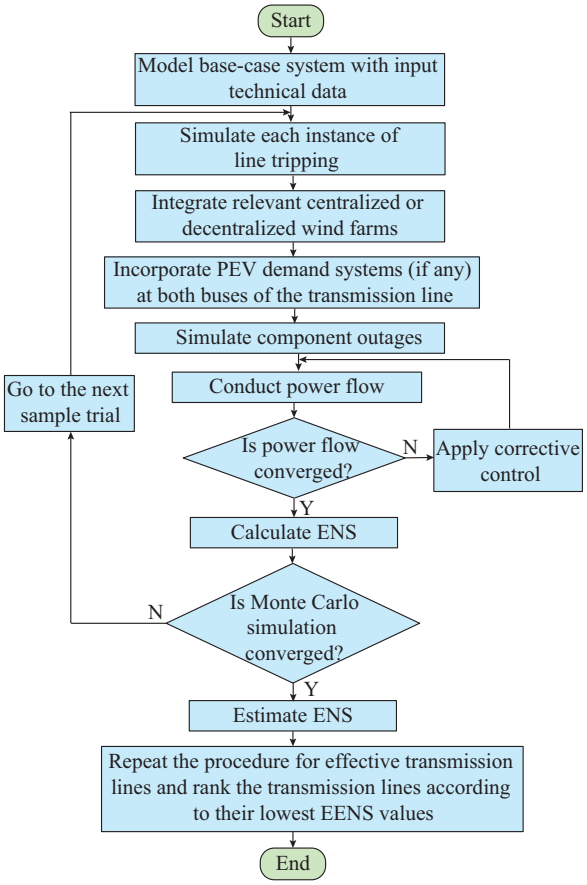


Fig. 1. Monte Carlo simulation in the first stage of proposed framework.

As shown in Fig. 2, the goal of the second stage is to assess the impact associated with strategic PEV charging locations when DTLs are applied on the transmission lines and wind farms are integrated.

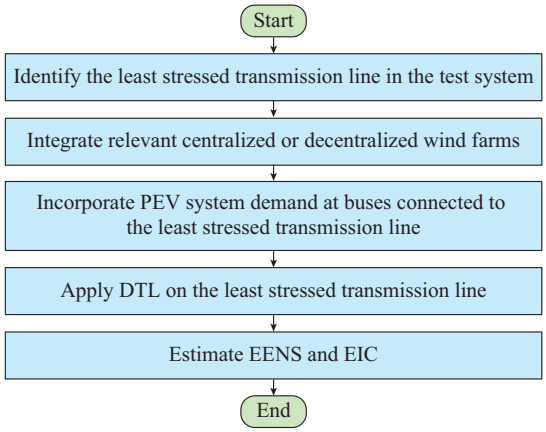


Fig. 2. Flowchart of the second stage of proposed framework.

### A. Modeling of Wind Power Generation

The model in [15] was simulated in MATLAB to generate the wind power generation profile considering (1):

$$P_W=\begin{cases}0 & 0\le V_w<V_{ci}\\ \left(A+BV_w+CV_w^2\right)P_{rated} & V_{ci}\le V_w<V_r\\ P_{rated} & V_r\le V_w<V_{co}\\ 0 & V_w\ge V_{co}\end{cases} \tag{1}$$

where $P_W$ is the total wind power generation; $V_w$, $V_{ci}$, $V_{co}$, and $V_r$ are the real-time, cut-in, cut-out, and rated wind speeds, respectively; $P_{rated}$ is the rated power output of the wind turbine; and $A$, $B$, and $C$ are the constant parameters calculated as in [15]. Equation (1) can be simplified as:

$$P_W=\left[K\left(A+BV_w+CV_w^2\right)+M\right]P_{rated} \tag{2}$$

where $K=1$ when $V_{ci}\le V_w<V_r$, and $M=1$ when $V_r\le V_w<V_{co}$, otherwise, $K$ and $M$ are equal to zero.

The centralized wind farm is integrated at the same bus for each scenario, and the decentralized wind farm is simultaneously integrated at three different buses, with the same equivalent capacity as that of the centralized wind farm. The buses considered for the integration of wind power generation are the load buses. In addition, these buses are connected to the transmission lines with the highest stress order to alleviate the system stress. Using the weather data for Birmingham, UK, in 2018, which is extracted from [16], 150 MW wind power generation is modeled. The installed capacity of the wind farm is less than 90% of that of the connected line rating in the IEEE 24-bus system. Figure 3 shows the wind power generation profile of a wind farm in Birmingham, UK, for a month in the winter in 2018.

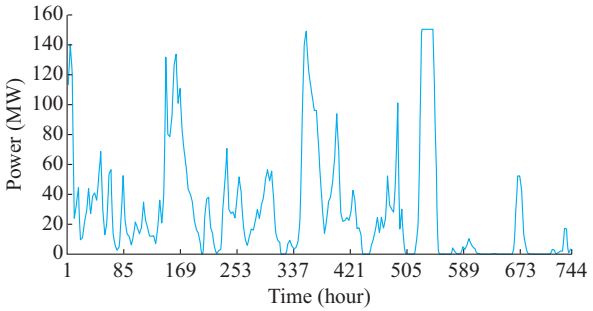


Fig. 3. Wind power generation profile of a wind farm in Birmingham, UK, for a month in winter.

### B. Modeling of PEV Charging

The PEV dataset from the UK Customer-Led Network Revolution Project [17] was employed to generate the PEV charging profile required for the test system. The hourly mean PEV charging demand for a typical day in winter in the UK is shown in Fig. 4. Figure 5 shows the hourly mean PEV charging demand for each month in the UK. The Monte Carlo simulation embedded in the proposed framework captures the charging demand at each hour (which covers the duration of a trial) from the temporal profile in Fig. 5. At the end of a simulation trial, the impact (ENS) is calculated to reflect the combinatorial effects of all processes, including the component outages, PEV charging, and intermittent wind power outputs. Different numbers of charging PEVs are considered for each scenario.

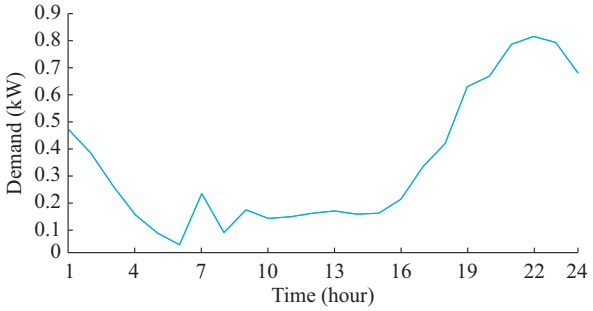


Fig. 4. Hourly mean PEV charging demand for a typical day in winter in UK.

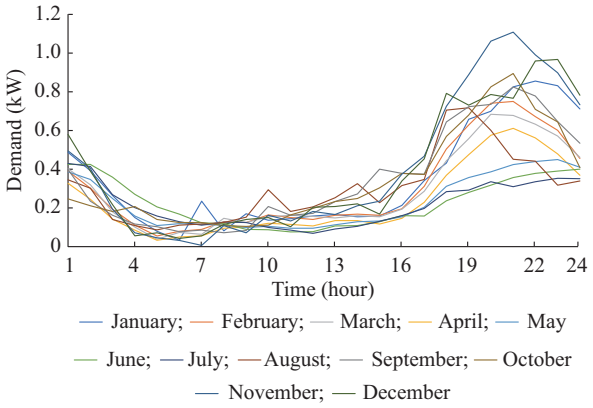


Fig. 5. Hourly mean PEV charging demand for each month in UK.

### C. Modeling of DTLs

To apply DTLs on the transmission lines in the test system, the DTL for a transmission line is calculated by applying the IEEE 738-2006 standard, considering the relevant weather conditions [6]. The required weather data are extracted from the UKCP2009 climate projections [18]. Random wind direction values (from 10 to 70 °C) are generated using a uniform random function. The IEEE 738-2006 standard relies on the heat equilibrium principle for the calculation of the thermal limit of the transmission line, using the following equations [6]:

$$H_G=H_L \tag{3}$$

$$q_s+I^2R\left(T_c\right)=q_c+q_r \tag{4}$$

where $H_G$ and $H_L$ are the heat gain and heat loss, respectively; $q_r$ and $q_c$ are the radiation and convection heat losses, respectively; $I$ is the line current; $R\left(T_c\right)$ is the line resistance at the line temperature $T_c$; and $q_s$ is the solar heat gain. The values of $q_c$, $q_r$, and $q_s$ are calculated according to the IEEE 738-2006 standard [6]

The thermal limit $TL_i$ for the transmission line is calculated as:

$$TL_i=I=\sqrt{\frac{q_c+q_r-q_s}{R\left(T_c\right)}} \tag{5}$$

Variations in the DTL are calculated as:

$$\Delta DTL_i(t) = \frac{DTL_i(t) - STL_i}{STL_i} \tag{6}$$

where $DTL_i(t)$ is the DTL at time $t$ for transmission line $i$; and $STL_i$ is the STL for transmission line $i$.

The DTL for the transmission line is calculated considering the weather conditions of Birmingham, UK, for one year. Figure 6 shows the DTL variations in a transmission line in January of a typical year. It also shows that for more than 85% of the time, the increase in DTL is more than 50% of the STL.

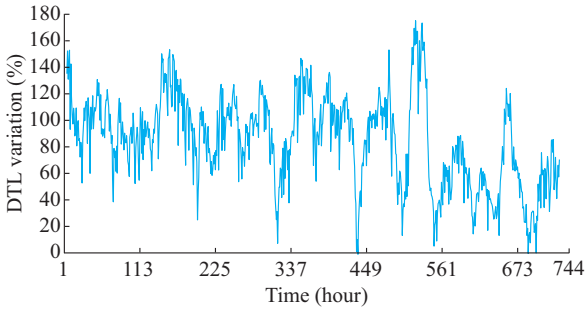


Fig. 6. DTL variations in a transmission line in January of a typical year considering weather conditions in Birmingham, UK.

### D. Estimation of Risk and Interruption Costs

The condition of an operating component is determined based on its failure rate and the generated random number. For each sample in the Monte Carlo simulation, multiple contingencies affecting the test system state are considered. The power flow is then run to check the technical feasibility of the test system. If the power system proves infeasible, remedial actions are applied to mitigate any violation problems, e. g., thermal overload, and to converge the power flow. First, re-dispatching of the generation in the network and transferring loads according to the lowest priorities of loads are executed to eliminate the overload. If these actions inadequately address the overload, load shedding is applied based on the load priority, with the lowest being shed first, to achieve convergence or eliminate violation problems in the test system. The load shedding is considered as an ENS to consumers, thus affecting the risk (of stress) index. The Monte Carlo simulation continues trial-by-trial until the convergence criteria are satisfied, with a minimum number of sample trials and a suitable degree of confidence. The minimum required number of samples considered in this study is 8760 (accounting for the number of hours in a year). The risk index is then calculated. In this study, the EENS represents the expected energy that cannot be delivered to the loads for any cause, including component failures or changes under operating conditions. It is a commonly used security indicator for assessing risk levels in a power system. In this context, EENS is used to measure the impact of STL and DTL applications on power systems with integrated wind farms and PEVs. For each trial in the Monte Carlo simulation, the ENS is calculated based on the time to restore the load and the magnitude of the disconnected load. The estimation of the EENS is calculated as [19]:

$$EENS = \frac{1}{n}\sum_{k=1}^{n} P_k T_k \tag{7}$$

where $n$ is the number of samples; $P_k$ is the value of the shedding load for sample $k$; and $T_k$ is the time required to restore the shedding load for sample $k$.

In the final step, EIC is calculated based on the ENS and the value of the lost load (VoLL) function [20]. The typical UK sector customer damage function [21] is used to reflect the VoLL. The EIC is calculated as:

$$EIC = \frac{1}{n}\sum_{k=1}^{n} ENS_k \cdot VoLL_{T_k} \tag{8}$$

where $ENS_k$ is the ENS for sample $k$; and $VoLL_{T_k}$ is the VoLL for the duration $T_k$.

## III. Case Studies

### A. Test System and Scenarios

To assess the performance of the proposed framework, the extended IEEE 24-bus system is simulated, as shown in Fig. 7 [14].

In the first stage, to rank the stressed transmission lines in the test system, the static performance of the framework is investigated through the application of STLs on the test system, considering the following scenarios.

1) Scenario A: each transmission line trip is simulated once in the test system, without any integration of the wind farm.

2) Scenario B: each transmission line trip is simulated once in the test system, with the integration of a centralized wind farm at Bus 10.

3) Scenario C: each transmission line trip is simulated once in the test system, with the integration of a centralized wind farm at Bus 8.

4) Scenario D: each transmission line trip is simulated once in the test system, with the integration of a centralized wind farm at Bus 6.

5) Scenario E: each transmission line trip is simulated once in the test system, with the integration of decentralized wind farms at Buses 10, 8, and 6.

6) Scenario F: PEV system demand is incorporated at the terminal buses of each transmission line at a time in the test system when no wind farm is integrated. In this scenario, 15000 PEVs are incorporated.

7) Scenario G: PEV system demand is incorporated at the terminal buses for each transmission line at a time in the test system when a decentralized wind farm is integrated at Buses 10, 8, and 6. In this scenario, 15000 PEVs are incorporated.

The purpose of the second stage is to assess the impact of strategic PEV charging locations with DTLs applied on the least stressed transmission line in a wind-integrated power system. The buses considered for the integration of wind farms are the load buses. As per the data in Table I, the stress orders of the transmission lines from the highest are 13, 12, 10, and 5, respectively. These transmission lines are connected to Buses 10, 8, and 6; thus, the integration of wind farms at these buses is expected to alleviate the system

stress in general theory. Six scenarios are established to verify the efficiency of the proposed framework, and in all of these scenarios, 5000-15000 PEVs are incorporated.

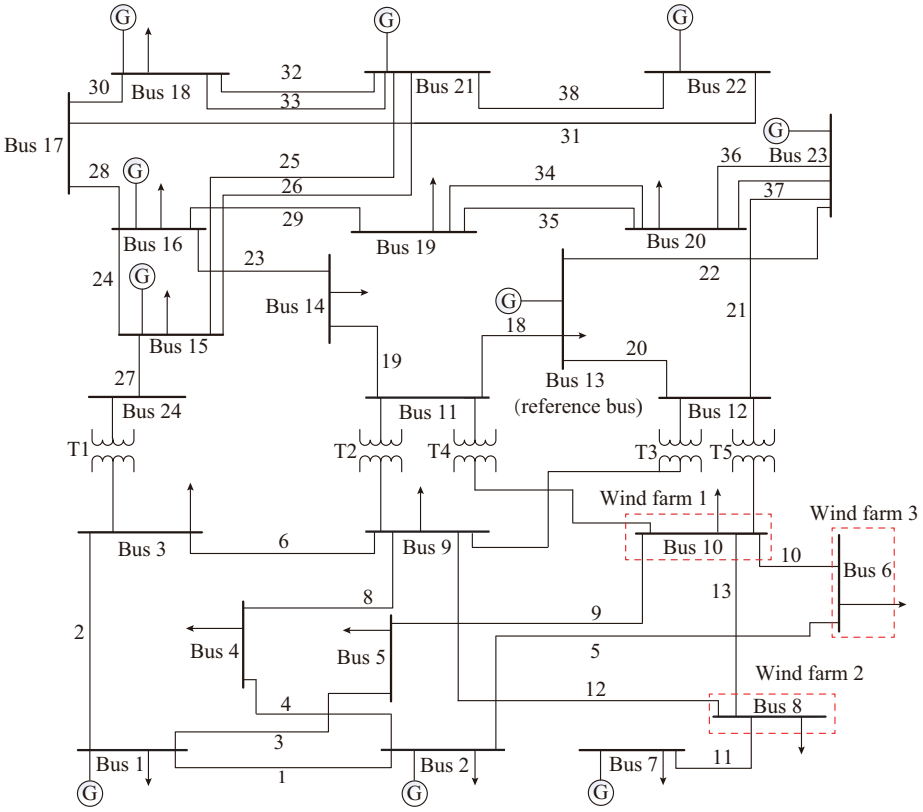


Fig. 7. Extended IEEE 24-bus system.

1) Scenario H: PEV system demand is incorporated at each bus of the least stressed transmission line at a time in the test system when STLs are applied on all transmission lines without any integration of wind farm.

2) Scenario I: PEV system demand is incorporated at each bus of the least stressed transmission line at a time in the test system when the DTLs are applied on the least stressed transmission line without any integration of wind farm.

3) Scenario J: PEV system demand is incorporated at each bus of the least stressed transmission line at a time in the test system when STLs are applied on all transmission lines with the integration of a decentralized wind farm at Buses 10, 8, and 6.

4) Scenario K: PEV system demand is incorporated at each bus of the least stressed transmission line at a time in the test system when the DTLs are applied on the least stressed transmission line with the integration of a decentralized wind farm at Buses 10, 8, and 6.

5) Scenario L: PEV system demand is incorporated at each bus of the highest stressed transmission line at a time in the test system when STLs are applied on all transmission lines without any integration of wind farm.

6) Scenario M: PEV system demand is incorporated at each bus of the highest stressed transmission line at a time in the test system when the DTLs are applied on the highest stressed transmission line without any integration of wind farm.

### *B. Results and Analysis*

Table I lists the stressed transmission lines in the test system ranked from the lowest to the highest stress (lowest to highest EENS value). The results presented in the table are for Scenarios A-G. It can be observed from the results that there is no change in the ranking for the first 8 transmission lines in Scenarios A-E. In contrast, transmission line 27 is ranked the 9$^{th}$ in Scenario A but the 23$^{rd}$ in Scenarios B-E and the rankings for other transmission lines differ by just one position in the wind power scenarios. According to the results of Scenarios F and G, a significant change in the ranking of the transmission line is evident compared with Scenario A. These findings indicate that the ranking of system stress is independent of the penetration level of the wind farm but is affected by the connection of PEV charging stations under *N*–1 security criteria.

The EENS and EIC for the scenarios without any integration of wind farm or PEV charging station are used as references to compare the results after those elements are added to the test system. Figures 8 and 9 show the changes in the EENS value with the application of STLs in the test system (Scenario H) and with the application of DTLs on the least stressed transmission line (transmission line 11, Scenario I), following the incorporation of PEV charging stations into the Buses 8 and 7 connected to transmission line 11. In general, the EENS value increases with the incorporation of PEV charging stations at both buses; however, the incorpora-

tion of PEV charging stations at Bus 8 results in a slightly lower EENS value compared with incorporation of PEV charging stations at Bus 7. When DTLs are applied on transmission line 11, the EENS value decreases when the number of PEVs is less than 10000. In addition, when DTLs are utilized in the least stressed transmission line, the EENS value in Scenario I is lower than that in Scenario H. Applying DTLs produces a significant reduction in the EENS value when PEV charging locations are selected strategically.

TABLE I
EENS-BASED RANKING OF STRESSED TRANSMISSION LINES

| Ranking | Transmission line | | | | | | |
|---|---|---|---|---|---|---|---|
| | A | B | C | D | E | F | G |
| 1 | 11 | 11 | 11 | 11 | 11 | 27 | 27 |
| 2 | 20 | 20 | 20 | 20 | 20 | 22 | 22 |
| 3 | 18 | 18 | 18 | 18 | 18 | 23 | 23 |
| 4 | 38 | 38 | 38 | 38 | 38 | 24 | 24 |
| 5 | 22 | 22 | 22 | 22 | 22 | 29 | 29 |
| 6 | 24 | 24 | 24 | 24 | 24 | 34 | 34 |
| 7 | 21 | 21 | 21 | 21 | 21 | 35 | 35 |
| 8 | 28 | 28 | 28 | 28 | 28 | 28 | 28 |
| 9 | 27 | 31 | 31 | 31 | 31 | 36 | 36 |
| 10 | 31 | 30 | 30 | 30 | 30 | 37 | 37 |
| 11 | 30 | 25 | 25 | 25 | 25 | 25 | 25 |
| 12 | 25 | 26 | 26 | 26 | 26 | 26 | 26 |
| 13 | 26 | 29 | 29 | 29 | 29 | 30 | 30 |
| 14 | 29 | 34 | 34 | 34 | 34 | 32 | 32 |
| 15 | 34 | 35 | 35 | 35 | 35 | 33 | 33 |
| 16 | 35 | 36 | 36 | 36 | 36 | 31 | 31 |
| 17 | 36 | 37 | 37 | 37 | 37 | 38 | 38 |
| 18 | 37 | 32 | 32 | 32 | 32 | 18 | 18 |
| 19 | 32 | 33 | 33 | 33 | 33 | 20 | 20 |
| 20 | 33 | 1 | 1 | 1 | 1 | 19 | 19 |
| 21 | 1 | 6 | 6 | 6 | 6 | 21 | 21 |
| 22 | 6 | 2 | 2 | 2 | 2 | 12 | 12 |
| 23 | 2 | 27 | 27 | 27 | 27 | 13 | 13 |
| 24 | 19 | 19 | 19 | 19 | 19 | 8 | 8 |
| 25 | 3 | 9 | 9 | 9 | 9 | 4 | 4 |
| 26 | 9 | 3 | 3 | 3 | 3 | 3 | 3 |
| 27 | 23 | 8 | 8 | 8 | 8 | 9 | 9 |
| 28 | 8 | 4 | 4 | 4 | 4 | 6 | 6 |
| 29 | 4 | 23 | 23 | 5 | 23 | 2 | 2 |
| 30 | 5 | 5 | 5 | 23 | 5 | 5 | 5 |
| 31 | 10 | 10 | 10 | 10 | 10 | 10 | 10 |
| 32 | 12 | 12 | 12 | 12 | 12 | 1 | 1 |
| 33 | 13 | 13 | 13 | 13 | 13 | 11 | 11 |

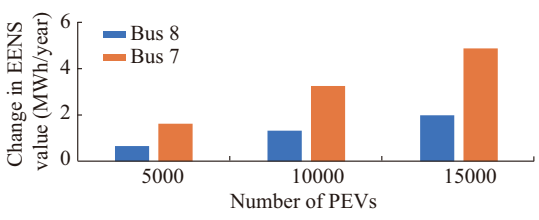


Fig. 8. Changes in EENS values for Scenario H.

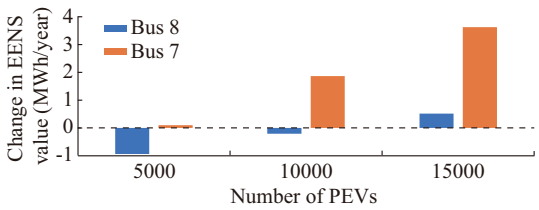


Fig. 9. Changes in EENS values for Scenario I.

Changes in the EIC for Scenarios H and I are shown in Figs. 10 and 11, respectively. It can be observed that the EIC decreases with the incorporation of PEV charging stations; however, a significant decline is evident in the EIC when DTLs are applied on transmission line 11, as indicated in Fig. 11. In both scenarios, Buses 8 and 7 exhibit the same reduction in EIC. Interestingly, the greatest decrease in EIC is observed when 15000 PEVs are incorporated according to Scenario I. The results reveal that the higher the number of PEVs in the system, the better the EIC performance might be due to the application of DTLs.

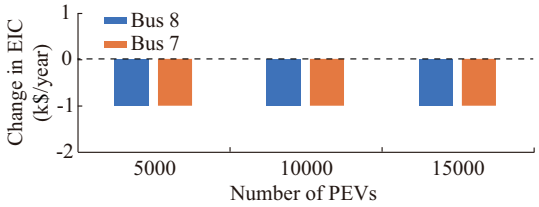


Fig. 10. Changes in EIC for Scenario H.

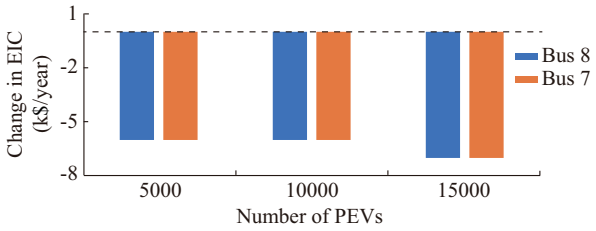


Fig. 11. Changes in EIC for Scenario I.

Figures 12 and 13 present the changes in EENS value resulting from Scenarios J and K, respectively. For both scenarios, the EENS value declines sharply with the integration of decentralized wind farms. The changes in EENS value follow a pattern similar to that of the scenario in which PEV charging stations are incorporated at both buses; however, the EENS value with the incorporation of PEV charging stations at Bus 8 is slightly lower than that for Bus 7. A small drop in the EENS value with Scenario K compared with that with Scenario J is evident as a result of the use of DTLs in the least stressed transmission line. Applying DTLs with the integration of a decentralized wind farm produces a significant reduction in EENS value when the PEV charging locations are selected strategically.

Figures 14 and 15 show the changes in EIC for Scenarios J and K, respectively. In both scenarios, a marked rise in EIC with the integration of a decentralized wind farm can be observed. A steep decrease in EIC is observed in Scenario K when applying DTLs on transmission line 11 compared with

Scenario J, especially when the number of incorporated PEVs is 15000, as shown in Fig. 15. The results reveal that as more PEVs are connected to an integrated decentralized wind farm, the application of DTLs results in a reduction of EIC when the PEV charging locations are selected strategically.

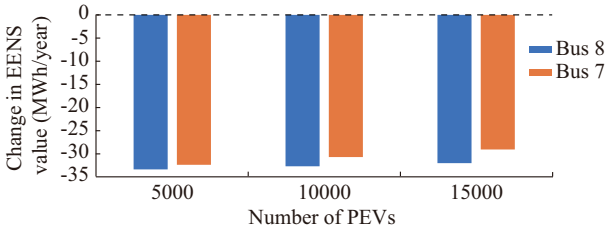


Fig. 12. Changes in EENS value for Scenario J.

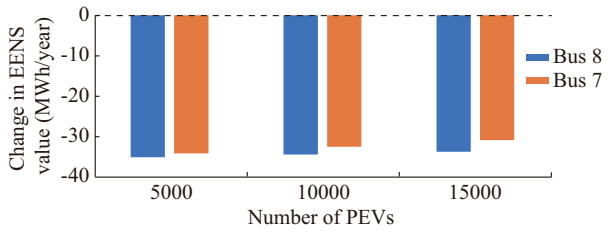


Fig. 13. Changes in EENS value for Scenario K.

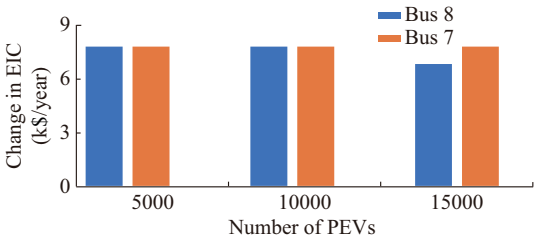


Fig. 14. Changes in EIC for Scenario J.

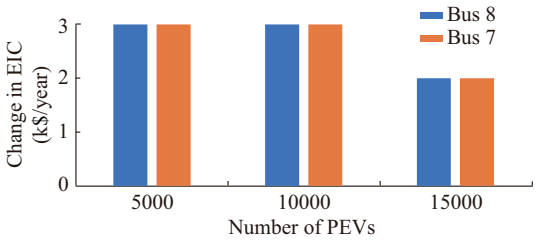


Fig. 15. Changes in EIC for Scenario K.

Figures 16 and 17 show the changes in EENS value with the application of STLs in the test system (Scenario L) and the application of DTLs on the highest stressed transmission line (transmission line 13, Scenario M), respectively, following the incorporation of PEV charging station at the Buses 8 and 10 connected to transmission line 13. In general, the EENS value increases with the incorporation of PEV charging stations at both buses; however, the incorporation of PEV charging stations at Bus 8 results in a slightly smaller EENS value compared with the effect at Bus 10. A significant increase is evident in the EENS value when DTLs are applied on the transmission line 13, as indicated in Fig. 17. Applying DTLs to the highest stressed transmission line produces a significant increase in the EENS value when PEV charging stations are incorporated.

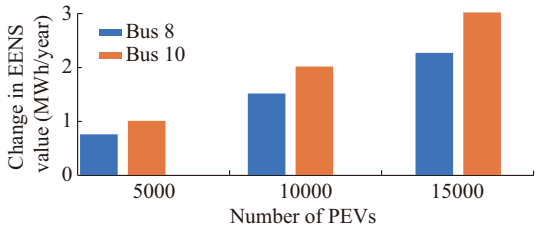


Fig. 16. Changes in EENS value for Scenario L.

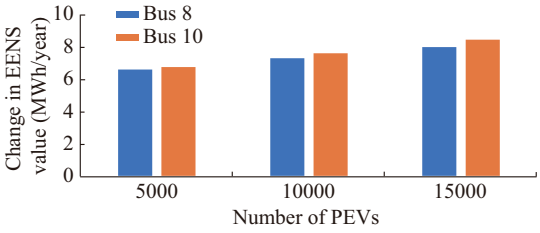


Fig. 17. Changes in EENS value for Scenario M.

Figures 18 and 19 show the changes in EIC for Scenarios L and M, respectively. It can be observed that the EIC decreases with the incorporation of PEV charging stations for Scenario L; however, when the PEV charging stations are incorporated at Bus 10, the EIC does not change when the number of PEVs is less than 10000. In Scenario M, there is a marked rise in the EIC when DTLs are applied on the transmission line 13. The results reveal that applying DTLs on the highest stressed transmission line produces worse EIC performance when PEV charging stations are incorporated.

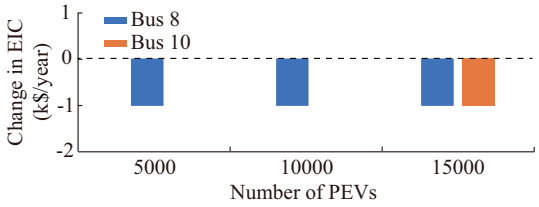


Fig. 18. Changes in EIC for Scenario L.

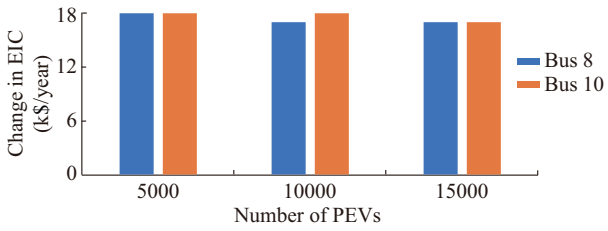


Fig. 19. Changes in EIC for Scenario M.

Changes in the EENS value and EIC for Scenarios I and M, when PEV charging stations are incorporated at Bus 8, are shown in Figs. 20 and 21, respectively. In both figures, a marked rise in the EENS value and EIC when DTLs are applied on the transmission line 13 can be observed; however, when DTLs are applied on the transmission line 11, the EENS value and EIC decrease. Applying DTLs produces a

significant reduction in the EENS value and a better performance of EIC when PEV charging locations are strategically selected.

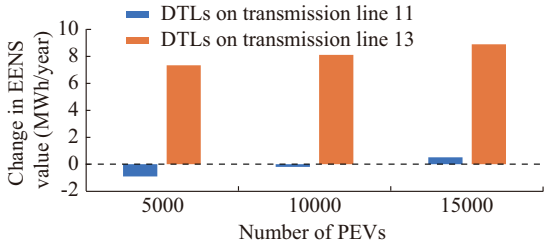


Fig. 20. Changes in EENS value for Scenarios I and M when PEV charging stations are incorporated at Bus 8.

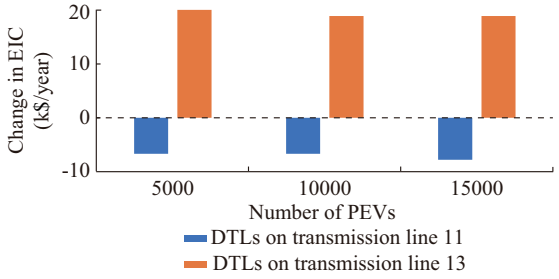


Fig. 21. Changes in EIC for Scenarios I and M when PEV charging stations are incorporated at Bus 8.

## IV. Conclusion

An innovative framework is proposed for assessing the impact of PEV charging locations in conjunction with applying DTLs to the least stressed transmission line and integrating wind farms. The framework considers the incorporation of the PEV charging demand at the terminal buses of the least stressed transmission line. The proposed framework also helps identify the strategic locations for mobile PEV charging stations.

The order of system stress is independent of the penetration level of wind power generation; however, it affects the strategic connection of PEVs under $N$–1 security criteria. It is notable that the application of DTLs with integrated decentralized wind farms significantly enhances the energy supply security and reduces the interruption costs when PEV charging stations are strategically located, considering the mobility of PEVs. The results also reveal that increments in the number of PEVs in the system are likely to reduce the EIC for systems that incorporate wind power generation and DTLs.

The proposed framework is useful for power system engineers in developing strategic operating plans to mitigate power system stresses with increased PEV connections.

## References

[1] D. A. Douglass, "Weather-dependent versus static thermal line ratings (power overhead lines)," *IEEE Transactions on Power Delivery*, vol. 3, no. 2, pp. 742-753, Apr. 1988.

[2] M. W. Davis, "A new thermal rating approach: the real time thermal rating system for strategic overhead conductor transmission lines–Part II: steady state thermal rating program," *IEEE Transactions on Power Apparatus and Systems*, vol. 96, no. 3, pp. 810-825, May 1977.

[3] M. W. Davis, "A new thermal rating approach: the real time thermal rating system for strategic overhead conductor transmission lines–Part I: general description and justification of the real time thermal rating system," *IEEE Transactions on Power Apparatus and Systems*, vol. 96, no. 3, pp. 803-809, May 1977.

[4] D. Douglass, W. Chisholm, G. Davidson *et al.*, "Real-time overhead transmission-line monitoring for dynamic rating," *IEEE Transactions on Power Delivery*, vol. 31, no. 3, pp. 921-927, Jun. 2016.

[5] R. Xiao, Y. Xiang, L. Wang *et al.*, "Power system reliability evaluation incorporating dynamic thermal rating and network topology optimization," *IEEE Transactions on Power Systems*, vol. 33, no. 6, pp. 6000-6012, Apr. 2018.

[6] *IEEE Standard for Calculating the Current-temperature of Bare Overhead Conductors*, IEEE Std 738-2006, 2006.

[7] B. Alharbi and D. Jayaweera, "Smart power system operation with dynamic thermal limits on critical transmission lines and integration of large PV systems," in *Proceedings of 2019 8th International Conference on Renewable Energy Research and Applications (ICRERA)*, Brasov, Romania, Nov. 2019, pp. 727-732.

[8] S. Rezaee, E. Farjah, and B. Khorramdel, "Probabilistic analysis of plug-in electric vehicles impact on electrical grid through homes and parking lots," *IEEE Transactions on Sustainable Energy*, vol. 4, no. 4, pp. 1024-1033, Sept. 2013.

[9] A. Almutairi and M. M. Salama, "Assessment and enhancement frameworks for system reliability performance using different PEV charging models," *IEEE Transactions on Sustainable Energy*, vol. 9, no. 4, pp. 1969-1984, Mar. 2018.

[10] L. Cheng, Y. Chang, J. Lin *et al.*, "Power system reliability assessment with electric vehicle integration using battery exchange mode," *IEEE Transactions on Sustainable Energy*, vol. 4, no. 4, pp. 1034-1042, Sept. 2013.

[11] D. Jayaweera and S. Islam, "Risk of supply insecurity with weather condition-based operation of plug in hybrid electric vehicles," *IET Generation, Transmission & Distribution*, vol. 8, no. 12, pp. 2153-2162, Dec. 2014.

[12] Y. Xiang, J. Liu, W. Yang *et al.*, "Active energy management strategies for active distribution system," *Journal of Modern Power Systems and Clean Energy*, vol. 3, no. 4, pp. 533-543, Oct. 2015.

[13] O. Sadeghian, M. Nazari-Heris, M. Abapour *et al.*, "Improving reliability of distribution networks using plug-in electric vehicles and demand response," *Journal of Modern Power Systems and Clean Energy*, vol. 7, no. 5, pp. 1189-1199, Sept. 2019.

[14] C. Grigg, P. Wong, P. Albrecht *et al.*, "The IEEE reliability test system-1996: a report prepared by the reliability test system task force of the application of probability methods subcommittee," *IEEE Transactions on Power Systems*, vol. 14, no. 3, pp. 1010-1020, Aug. 1999.

[15] P. Giorsetto and K. F. Utsurogi, "Development of a new procedure for reliability modeling of wind turbine generators," *IEEE transactions on Power Apparatus and Systems*, vol. PAS-102, no. 1, pp. 134-143, Jan. 1983.

[16] D. Jacob, J. Petersen, B. Eggert *et al.*, "EURO-CORDEX: new high-resolution climate change projections for European impact research," *Regional Environmental Change*, vol. 14, no. 2, pp. 563-578, Mar. 2014.

[17] R. Wardle, K. A. Capova, P. Matthews *et al.* (2015, Jan.). Insight report electric vehicles. [Online]. Available: http://www.networkrevolution.co. uk/wp-content/uploads/2015/01/CLNR-L092-Insight-Report-Electric-Vehicles.pdf

[18] P. Jones, C. Harpham, C. Kilsby *et al.* (2010, Jul.). UK climate projections science report: projections of future daily climate for the UK from the weather generator. [Online]. Available: https://ueaeprints.uea.ac.uk/id/eprint/34292/

[19] D. Jayaweera and S. Islam, "Security of energy supply with change in weather conditions and dynamic thermal limits," *IEEE Transactions on Smart Grid*, vol. 5, no. 5, pp. 2246-2254, Sept. 2014.

[20] K. Kariuki and R. N. Allan, "Evaluation of reliability worth and value of lost load," *IEE Proceedings: Generation, Transmission and Distribution*, vol. 143, no. 2, pp. 171-180, Mar. 1996.

[21] R. Allan and R. Billinton, "Probabilistic assessment of power systems," *Proceedings of the IEEE*, vol. 88, no. 2, pp. 140-162, Feb. 2000.

**Bader Alharbi** received the B.Sc. degree in electrical engineering from Qassim University, Buraydah, Saudi Arabia, and the M.Eng. degree in electrical and computer engineering from Concordia University, Montreal, Canada. He is a Lecturer in Department of Electrical in Majmaah University, Al-Majmaah, Saudi Arabia, since 2016, and currently working towards his Ph. D.

degree at the Department of Electronic, Electrical and Systems Engineering in University of Birmingham, Birmingham, UK. His research interests include risk, reliability, and security assessment of smart grids.

**Dilan Jayaweera** received the Ph.D. degree in electrical power engineering from the University of Manchester Institute of Science and Technology (UMIST), Manchester, UK, in 2003. He is currently a Senior Lecturer in electrical power systems with the Department of Electronic, Electrical, and Systems Engineering (EESE), University of Birmingham, Birmingham, UK. He is also a Chartered Engineer in UK, a Chartered Professional Engineer in Australia, and a Fellow at Engineers, Australia. He is also an editor of IEEE Transactions on Power Systems and Power Engineering Letters. He has wide experiences in energy industry, research, and teaching. He has authored a significant number of research articles in scientific journals, conference proceedings, and as book chapters in the fields of power system security, reliability, active distribution network operation, smart grids, smart asset management, microgrids, and risks in power systems.